A Flight Control System design for an Unmanned Helicopter

Soohong Park*, Jongkwon Kim **, Cheolsoon Jang***

* Department of Mechatronics Engineering, Dongseo University, Sasang Ku, Pusan 617-716, Korea
(Tel : 82-51-320-1765; Fax : 82-51-320-1751 ; E-mail:shpark@donseo.ac.kr)
** Department of Mechatronics Engineering, Dongseo University, Sasang Ku, Pusan 617-716, Korea
(Tel : 82-51-320-1765; Fax : 82-51-320-1751 ; E-mail:joinkiss@korea.com)
*** Shin Dong Digitech Co., Ltd., 3F, Jinyoung Bldg, 1213-1, Choryang-1 Dong, Pusan 601-839, Korea
(Tel : 82-51-510-2309; Fax : 82-51-513-3760 ; E-mail:csjang@shindong.com)

Abstract: Unmanned Helicopter has several abilities such as vertical Take off, hovering, low speed flight at low altitude. Such vehicles are becoming popular in actual applications such as search and rescue, aerial reconnaissance and surveillance. These vehicles also used under risky environments without threatening the life of a pilot. Since a small aerial vehicle is very sensitive to environmental conditions, it is generally known that the flight control is very difficult problems. In this paper, a flight control system was designed for an unmanned helicopter. This paper was concentrated on describing the mechanical design, electronic equipments and their interconnections for acquiring autonomous flight. The design methodologies and performance of the helicopter were illustrated and verified with a linearized equation of motion. The LQG based estimator and controller was designed and tested for this unmanned helicopter.

Keywords: Flight Controller, Unmanned Helicopter, DSP(Digital Signal Processor), LQG(Linear Quadratic Gaussian) Control

1. Introduction

The unmanned aerial vehicles (UAV) are remotely piloted or self-piloted aircraft. Recently, their abilities are much more that they carry cameras, sensors, communications equipment, or other payloads. Some day several UAV are operated in military purposes such as reconnaissance, surveillance, and intelligence of enemy forces without risking the lives of an aircrew. These actual applications need more versatile performance. Among these abilities hovering and vertical take off ability are necessarily needed. The helicopter can flight by resulting lifting force of large radius main rotor. For the single rotor helicopter, it use tail rotor to prevent body rotation. Thus the two state variables, azimuth angle and elevation angle, are strongly coupled, and have characteristics of typical MIMO system. The hovering capability of small helicopters can potentially be used in actual application. It is necessary to design a feedback control system with adequate closed loop bandwidth. This paper was concentrated on describing the mechanical design, electronic equipments and their interconnections for acquiring autonomous flight. The equations of motion were derived by the general Newton-Equation for a rigid body. The design methodologies and performance of the helicopter were illustrated and verified with a linearized equation of motion. The LGQ based estimator and controller was designed and tested for this unmanned helicopter.

2. Modeling of the Unmanned Helicopter

2.1. Equation of Motion for a Rigid Body

It is generally used the body axis coordinate system to describe the equation of motion for vehicles.
If this coordinate system is considered, the Newton-Euler equation for rigid body is the form.

$$\begin{bmatrix} mI & 0 \\ 0 & J \end{bmatrix} \begin{bmatrix} \dot{v}^b \\ \dot{\omega}^b \end{bmatrix} + \begin{bmatrix} \omega^b \times mv^b \\ \omega^b \times J\omega^b \end{bmatrix} = \begin{bmatrix} f^b \\ \tau^b \end{bmatrix} \tag{1}$$

where, $\dot{v}^b$ is the acceleration with respect to the center of mass, $\dot{\omega}^b$ is the angular acceleration with respect to the center of mass, J is moment of inertia, f^b is external force, and τ^b is external moment, respectively. The resulting nonlinear equation can be represented by the following equations.

$$\begin{aligned} \dot{v}^b &= \frac{1}{m}\left(f^b - \omega^b \times v^b\right) \\ \dot{\omega}^b &= J^{-1}\left(\tau^b - \omega^b \times J\omega^b\right) \end{aligned} \tag{2}$$

The equations of motion can be decomposed by the force and moment components at center of mass of the body.

$$\begin{aligned} f_X &= m(\dot{u} + wq - vr) \\ f_Y &= m(\dot{v} + ur - wp) \\ f_Z &= m(\dot{w} + vp - uq) \end{aligned} \tag{3}$$

$$\begin{aligned}\tau_R &= \dot{p}I_{xx} - \dot{r}I_{xz} + qr(I_{zz} - I_{yy}) + pqI_{xz} \\ \tau_M &= \dot{q}I_{yy} + pr(I_{xx} - I_{zz}) + (p^2 - r^2)I_{xz} \\ \tau_N &= \dot{r}I_{zz} - \dot{p}I_{xz} + pq(I_{yy} - I_{xx}) + qrI_{xz}\end{aligned} \quad (4)$$

The external forces and moments acting the body can be summarized as the forms.

$$f^b = \begin{bmatrix} X_M + X_T + X_H + X_V + X_F \\ Y_M + Y_T + Y_H + Y_V + Y_F \\ Z_M + Z_T + Z_H + Z_V + Z_F \end{bmatrix} + R^T \begin{bmatrix} 0 \\ 0 \\ mg \end{bmatrix} \quad (5)$$

$$\tau^b = \begin{bmatrix} R_M + R_F \\ M_M + M_T + M_F \\ N_M + N_F \end{bmatrix} = \begin{bmatrix} Y_M h_M + Z_M y_M + Y_T h_T + Y_V h_V + Y_F h_F \\ -X_M h_M + Z_M l_M - X_T h_T + Z_T l_T - X_H h_H + Z_H l_H - X_V h_V \\ -Y_M l_M - Y_T l_T - Y_V l_V - T_F l_F \end{bmatrix} \quad (6)$$

where, the subscripts M, T, H, V and F mean the main blade, the tail blade, the horizontal stabilizer, the vertical stabilizer and body frame, in order. And R represents the transformation matrix for Euler attitude angles.

2.2. Equation of Motion for Hovering

It is reasonable that the drag terms can be negligible at hovering or low speed level flight. Thus, the above equations can be abbreviated as the following nonlinear equations.

$$\begin{aligned} X_M &= T_M \sin(a_{1sM} + i_M) \\ Y_M &= T_M \sin(b_{1sM}) \\ Z_M &= -T_M \cos(a_{1sM} + i_M) \\ R_M &= \left(\frac{dR}{db_{1sM}}\right) b_{1sM} - Q_M \sin(a_{isM} + i_M) \\ M_M &= \left(\frac{dR}{da_{1sM}}\right) a_{1sM} + Q_M \sin(b_{1sM}) \\ N_M &= Q_M \cos(a_{1sM} + i_M)\cos(b_{1sM}) \\ M_T &= -Q_T \quad , \quad Y_T = -T_T \quad , \quad Z_T = T_T b_{1aM} \end{aligned} \quad (7)$$

If the equilibrium conditions are applied for above equation, the nonlinear equations are derived.

$$\ddot{x} = -\frac{T_M \sin(a_{1sM} + i_M)}{m} - g\sin\theta + \dot{y}r - \dot{z}q \quad (8)$$

$$\ddot{y} = \frac{T_M \cos(b_{1sM}) + T_T}{m} + g\sin\phi - \dot{x}r + \dot{z}p \quad (9)$$

$$\ddot{z} = \frac{-T_M \cos(a_{1sM} + i_M) + T_m\left(\frac{D_v}{mg}\right)_H + T_M\left(\frac{D_v}{mg}\right)_F}{m} + g\sin\theta - \dot{x}q + \dot{y}p \quad (10)$$

$$\dot{p} = \frac{1}{I_{xx}}\left(\left(\frac{dR}{db_{1sM}}\right) b_{1sM} + T_M \cos(b_{1sM}) h_M - T_M \cos(a_{1sM} + i_M) y_M + T_T h_T\right) + \frac{(I_{yy} - I_{zz})}{I_{xx}} qr \quad (11)$$

$$\dot{q} = \frac{1}{I_{yy}}\left(\left(\frac{dM}{da_{1sM}}\right) a_{1sM} + T_M \sin(a_{1sM} + i_M) h_M + Q_T - T_M \cos(a_{1sM} + i_M) l_M + T_M\left(\frac{D_v}{mg}\right)_H l_H + T_M\left(\frac{D_v}{mg}\right)_F l_F\right) + \frac{(I_{zz} - I_{xx})}{I_{yy}} pr \quad (12)$$

$$\dot{r} = \frac{1}{I_{zz}}(Q_M - l_T T_T) + \frac{(I_{xx} - I_{yy})}{I_{zz}} pq \quad (13)$$

3. System Design of the Unmanned Helicopter

3.1. Structural Design

AutoCAD-2000 and CATIA-V6 were used for this structural Design. And the system parameters were also derived by using these computer tools. The test helicopter has four blades teetering rotor augmented with direct head system. Figure 1 represents that the overall 2-D structure design of the unmanned Helicopter. Rotor speed range is 750-820 RPM. Two electronic governors maintain commanded rotor speed by adjusting throttle commands. Figure 2 represents the assembled whole unmanned helicopter. Figure 3 represents the mechanical structures of main and tail rotor system. Two G800BPU 2 cycle piston valve type gasoline engines are used for the power system. Figure 4 illustrates the structure of mount, gear box and torque curve of the engine.

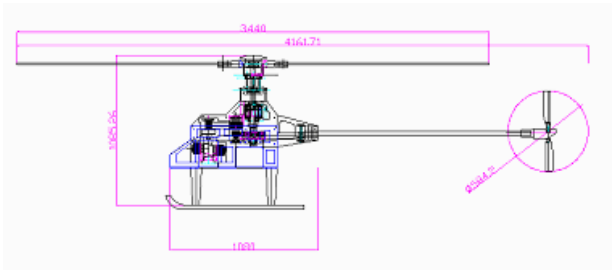

Fig. 1. 2-D Design of Unmanned Helicopter

Fig. 2. Assembled Unmanned Helicopter

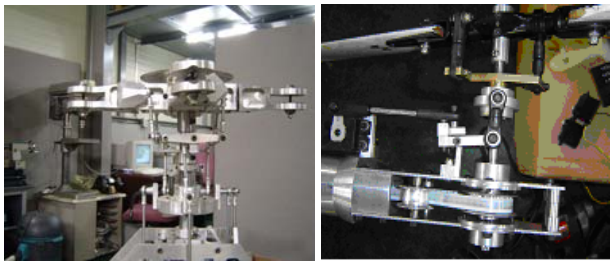

Fig. 3. Structure of Main Rotor and Tail Rotor

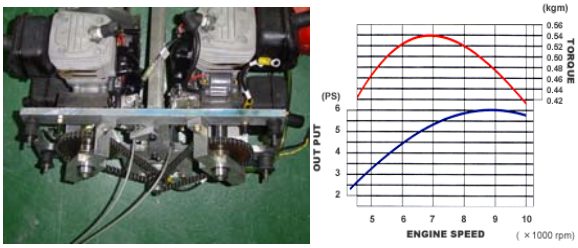

Fig. 4. Mount, gear box and Torque Curve of G800BPU Engine

3.2. Aerodynamic Design

To calculate the thrust of main rotor, the non-steady uniform strength source-doublet panel method was used. By using this panel method, downstream and thrust was calculated. To illustrate distortions of the downstream, vortex lattice method was used for the calculation of downstream rollup. Vortex core model of Scully was also used to eliminate the singularity on the center of vortex. Also, to eliminate potential value of downstream panel which collided with blade, solid boundary condition would be satisfied when downstream panel was in wing. Figure 5 illustrate upper view of the main rotor blade, pressure distribution and wake shape at collective angle is 12°. Following figure 6 illustrates calculate thrust curve with respect to collective angles. About 100kgf of rotor thrust was produced at collective angle 8°. In spite of considering computational error, the calculation result was sufficient for the unmanned helicopter thrust. With increasing the collective angle, the more thrust can be acquired.

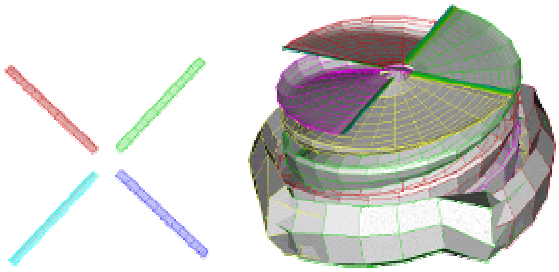

Fig. 5. Main Rotor Blade and Pressure Distribution and wake

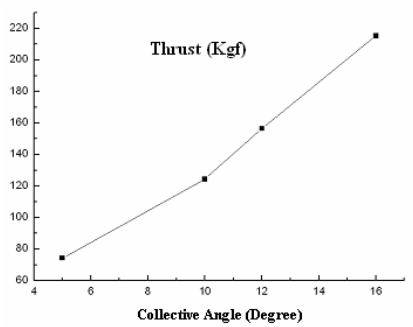

Fig. 6. Thrust Curve with respect to Collective Angles

3.3. Electronic Equipments

Figure 7 and 8 illustrate the structure and interconnections of the on-board avionics such as main processing unit, sensors, servos, and so on. The DSP controls the most of the calculation and processing work. Next chapter described more detailed specifications of the DSP. In order to facilitate helicopter recovery in case of CPU or min battery failure, a separate microprocessor powered from a different power source handles the task of driving the servo actuators. Flight sensors were chosen such that all relevant state vector elements can be estimated with reasonable bandwidth of the observer. Fast and powerful servos must be chosen for all channels. This helicopter was equipped with fast Seiko PS-050 servos. PS-050 is a precision electro-mechanical servo motor for radio control applications such as the servo for RPV, UAV & UVS project; industrial and special effects robotics ruggedly designed and built for hostile environments and performance-critical applications. During normal automated control operation, the microprocessor receives serial commands from the DSP and converts them to five PWM signals.

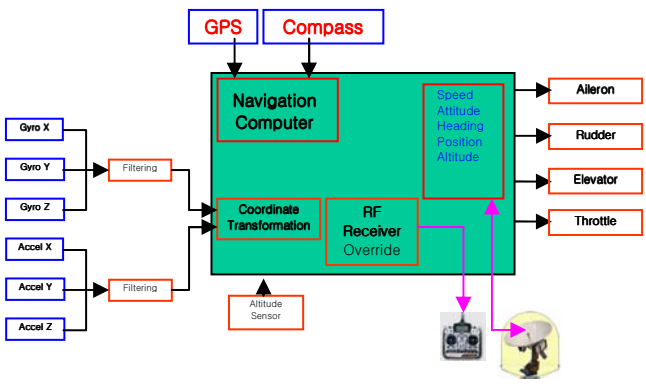

Fig. 7. Function Diagram of Unmanned Helicopter System

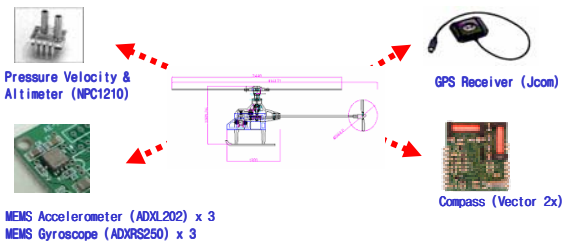

Fig. 8. On Board Sensors

Note that the gyro biases drift over time, and this drift turns out to be significant for our duration of flight. Once per second measurement updates are available from GPS(2D inertial position and velocity), barometric altimeter, and magnetic compass. Yaw rate bias can be compensated for by the compass magnetic heading measurement. GPS vertical velocity, altitude, and pressure altitude are used essentially to compensate for vertical accelerometer bias. The helicopter attitude can be estimated to within 1 deg for around 1 minute, which provides plenty of time for safety pilot to switch to manual control. The full scale of was chosen at +/- 300deg/sec to enable high-rate maneuvers around any axis. The GPS receiver gives 1 Hz updates of the 2D inertial position and velocity. The magnetic compass senor is used to measure three components of earth magnetic field in proportion to body axis. The barometric altimeter is used to provide additional altitude information. This is an absolute pressure sensor with the range 0-15 psi. The resolution is 0.005psi, which is 10ft.

3.4. Main Controller

The Texas Instrument DSP Controller (TMS320F241), developed for 'Motion Control Chip' is used for calculation and processing controller for these experiments. This controller is 16 bit high speed Processor. It has 6 PWM (Pulse Width Modulation), 12 bit timer and 10 channel 10bit AD converter. Also it has a QEP input devices for position senor, capture device and external interrupt devices. Thus, this processor is suitable for motion control with motor and an excellent DSP controller having good performance with low price. Figure 6 illustrates the event manager module and its functional block diagram of the DSP controller. The followings are the specification of the DSP (TMS320F241) controller

- 544 Word ×16 Bits의 on-Chip DARAM
- 8K Words×16 Bits의 Flash EEPROM
- Event Manager Module
- 8 Compare/PWM Channel
- 2 16-it General-Purpose Timers
- 3 16-Bit Full Compare Units With Deadband
- 3 Capture(2 QEP Interface)
- 1 10-Bit ADC With 8 Multiplexed Channels
- 26 General-Purpose I/O
- Watchdog Timer
- Serial Communications Interface (SCI)
- 16-Bit Serial Peripheral Interface(SPI)
- 5 External Interrupts
- 3 Power-Down Mode for Low-Power
- Scan-Based Emulation(JTEG)
- Code Composer Studio(IDE)

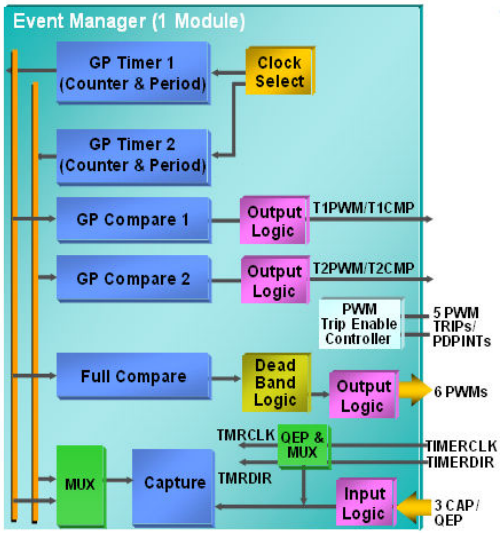

Fig. 9. EVM Block Diagram of a DSP controller

3.5. Attitude Control

For multivariable and highly decoupled system such as helicopter, The LQG based controller provides excellent robustness to modeling errors. This is essential, such it is rather difficult to model or identify rotorcraft dynamics accurately, especially in fast forward flight. In this paper, the perturbation method was applied for the nonlinear equation (8)-(13) to acquire the linearized equation at hovering equilibrium condition. The resulting equations are general state space forms.

$$\dot{X} = AX + BU \qquad (14)$$
$$Y = CX + DU$$

The states and control inputs are selected by the following forms.

$$X = [u, v, w, \phi, \theta, p, q, r] \qquad (15)$$
$$U = [\delta_c, \delta_e, \delta_a, \delta_r]$$

The state values are, three velocity components, roll and pitch angle, and roll, yaw, pitch rates, in order. Based on this linearized equation, the LQG control scheme is applied. This control theory is engineering method for general LQG control

theory, which is well known to provide excellent robustness to modeling errors. The LQG based mulitivariable controller is suitable for a helicopter flight control system. This controller has Kalman filer for state estimation and has compensator gain for optimal control. Figure 10 represents roll, pitch and yaw angles responses when initial value of pitch angle is 0.2 radian. This figure shows that the responses are good enough for real-time control for the designed unmanned helicopter.

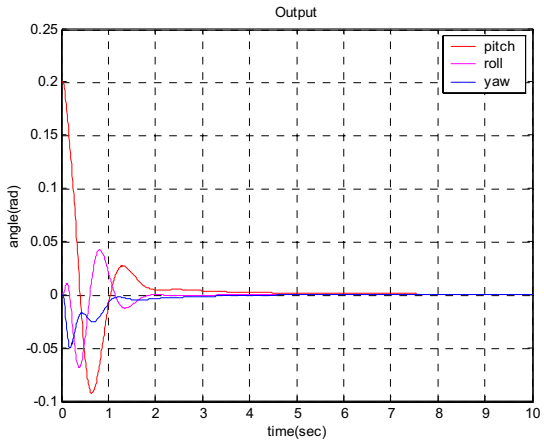

Fig. 10. attitude response at initial pitch angle = 0.2 radian

4. Conclusions and Further Research

Computer based design and simulation for the unmanned helicopter was performed. System configuration and interference was also tested for the designed unmanned helicopter. And a flight controller was implemented a DSP based controller. A multivariable controller was designed, tested and verified with computer simulation. Three attitude angle responses were reasonable for unmanned helicopter and will be useful for advanced embedded platform. Next step on the way to autonomous helicopter is to create a well designed test procedure, GCMS(Ground Control and Monitoring System) and a linearized wide-areas model, adequate for control law design. And the nonlinear model will be used in the hardware-in-the-loop simulation to check out control software. The state estimation method such as Kalman filter is required for robust to short GPS outages. Also, it is required that the real time OS(operating system) is implemented to autopilot computer for graphical interface and it is necessary that the communication with the ground station via a wireless system. It will give more convenient environments to further research. The state estimation method such as Kalman filter is required for robust to short GPS outages.

References

[1] J. G. Leishman, “Principles of Helicopter Aerodynamics”, Cambridge Aerospace Series, Cambridge University Press, 2000.

[2] S. Newman, “The Foundations of Helicopter Flight”, Edward Arnold, 1994

[3] MIL-H-8501, "Helicopter Flying and Ground Handling Qualities, General Requirements for", 1962.

[4] Aeronautical Design Standard -33C, "Handling Qualities Requirements for Military Rotorcraft", 1989.

[5] DARCOM-CP-2222-S10000J, "Prime Item Development Specification for UH-60 BlackHawk"

[6] M.F. Weilenmann, H,O. Geering, “A Test Bench for Rotorcraft Hover Control”, Proc. AIAA Guidance, Navigation and Control Conference, pp1372-1382, 1993.

[7] Raymond W. Prouty, *Helicopter Performance, Stability, and Control*, 1986

[8] *Federal Aviation Regulations(FAR), Part 29, Airworthiness. Standards : Transport Category Rotorcraft*, 1993.

[9] *Rotorcraft Design for Operations, AGARD-CP-423*, 1986

[10] *Engineering Design Handbook - Helicopter Engineering, Part Ⅰ, Preliminary Design, AMCP 706-210, Dept. of the Army, Headquarters United States Army Material Command,* 1974.

[11] *Engineering Design Handbook - Helicopter Performance Testing, AMCP 706-204, Dept. of the Army, Headquarters United States Army Material Command*, 1974.

[12] Texas Instruments(TI), *S320F243/F241/C242 DSP Controllers Reference Guide, SPRU276C*, 2000.

[13] B. L. Steven and F. L. Lewis, Aircraft Control and Simulation, A Wiley-Interscience Publication, 1992.

[14] D.G.Thompson and R. Bradley, “Mathematical Definition of Helicopter Maneuvers”, Journal of American Helicopter Society, October, 1997, pp307-309.

[15] Dave P. Witkowski, Alex K. H. Lee, and John P. Sullivant, "Aerodynamic Interaction Between Propellers and Wings", J. Aircraft, Vol. 26, No. 9 ,1989

[16] J. Katz and A. Plotkin, "Low Speed Aerodynamics from Wing Theory to Panel Methods", McGraw-Hill, INC., 1991.

[17] F. T. Johnson, "A General Panel Method for the Analysis and Design of Arbitrary Configurations in Incompressible Flows", NASA Contractor Report 3079, 1980.

[18] Qin E, Guowei Yang, and Fengwei Li, "Numerical Analysis of the Interference Effect of Propeller Slipstream on Aircraft Flowfield", J. Aircraft, Vol. 35, No. 1, 1998.